IOSR Journal of Applied Chemistry (IOSR-JAC)
e-ISSN: 2278-5736.Volume 17, Issue 4 Ser. 1 (April 2024), PP 25-34
www.iosrjournals.org

Co_3BaNiO_6Nanoparticles For Enhanced Photocatalytic Degradation Of Toluidine Blue

Jinesh Menaria[1], Dushyant Kumar Prajapati[2], Jeevan Kunwar Chouhan[3], Tejveer Singh Tomar[4], Shipra Bhardwaj*[5]
[1, 2, 3, 4,* 5]*government Meera Girls' College, Mohan Lal Shukhadia University, Udaipur, Rajasthan, India*

***Abstract**:*
The synthesis of a novel nanoparticle Co_3BaNiO_6, utilizing co-precipitation method is carried under controlled conditions. Structural and morphological properties of the as synthesized material are meticulously characterized through X-ray diffraction (XRD), field-emission scanning electron microscopy (FE-SEM) etc. techniques. Furthermore, we investigated the impact of calcination temperature on the morphology of the nanomaterial. UV–Vis spectroscopy revealed a peak absorbance at 232nm, with an optical bandgap estimated to be ≈4.3eV.Subsequently, the synthesized nanoparticles (NPs) are then employed as catalyst for the photodegradation of Toluidine blue (TB) dye. A systematic kinetic investigation is conducted to extract maximum degradation conditions. Remarkably, Co_3BaNiO_6 exhibited significant degradation efficiency, achieving approximately 89%degradation within a 40-minute timeframe. Optimal degradation performance was attained at pH 10.5, catalyst dosage of 0.18g, initial dye concentration of $0.4X10^{-4}$ ppm accompanied by a light intensity of 1640 mW/cm^2.Moreover, we assessed the recyclability of the photocatalyst up to five cycles with negligible loss in efficiency. These findings underscore the potential of Co_3BaNiO_6 nanoparticles as promising photocatalyst for the treatment of water contaminated with organic dyes.

***Keywords:**Photocatalysis, Photodegradation, Coprecipitation, Dye Degradation, Water treatment.*

Graphical Abstract:

Date of Submission: 17-04-2024 Date of Acceptance: 27-04-2024

I. Introduction

Water, an irreplaceable natural resource, is facing a dire threat due to widespread pollution stemming from factors like rapid industrialization, urbanization, sewage leakage etc. The indiscriminate discharge of hazardous industrial wastes into water bodies poses a significant risk to water quality [1]. Among the array of pollutants contaminating aquatic ecosystems, dyes, heavy metals, pesticides, and pharmaceuticals stand out as major culprits [2]. Urgent measures are imperative for the removal or degradation of these pollutants to avert environmental hazards.Dyes, in particular, present a formidable challenge, necessitating effective methods for their elimination from wastewater. Several techniques such as adsorption, cation exchange, electrochemical degradation, biological treatment, solvent extraction, and advanced oxidation processes have been employed for this purpose [3]. However, while these methods exhibit efficacy in removing organic contaminants, they often fall short of complete destruction.

In this context, photodegradation has emerged as a promising modern approach for tackling water pollution. Extensive research endeavors have been dedicated to exploring this technique, which not only facilitates the removal of toxic pollutants but also their transformation into non-toxic byproducts. Photodegradation entails the breakdown of complex organic substances into simpler, less harmful molecules of lower molecular weight, facilitated by light and a photocatalyst [4].

Cobalt-based oxide nanoparticles have garnered significant attention in recent years due to their remarkable catalytic properties and wide-ranging applications, particularly in environmental remediation. Among these, cobalt oxide (CoO) and cobalt sesquioxide (Co_2O_3) nanoparticles have emerged as promising candidates for the degradation of various organic pollutants, including synthetic dyes commonly found in industrial effluentsowing to their unique electronic structures and high surface areas. These nanoparticles can effectively generate reactive oxygen species (ROS) upon irradiation with light, which play a crucial role in the degradation of organic pollutants through oxidative processes. Furthermore, the facile synthesis and tunable physicochemical properties of cobalt oxide-based nanoparticles offer versatility and customization for specific applications in dye degradation.Several studies have reported the successful application of cobalt oxide and cobalt sesquioxide nanoparticles in the degradation of a wide range of dyes, including azo dyes, anthraquinone dyes, and triarylmethane dyes [5].

Barium oxide nanoparticles, with their high surface area and unique physicochemical properties, offer favorable characteristics for catalytic degradation processes. These nanoparticles have demonstrated exceptional efficacy in promoting oxidative degradation reactions, making them promising candidates for the treatment of dye-containing wastewater. By harnessing their inherent catalytic activity, barium oxide nanoparticles can facilitate the breakdown of organic dyes into less harmful byproducts, thereby mitigating environmental pollution and safeguarding human health [6].Numerous studies have investigated the application of barium oxide nanoparticles for the degradation of various classes of organic dyes such as methylene blue [7],Malachite green [8] etc.

Nickel oxide nanoparticles exhibit exceptional catalytic activity, high surface area, and tunable surface chemistry, making them promising candidates for the degradation of organic dyes in aqueous environments. Leveraging their intrinsic photocatalytic properties, these nanoparticles can initiate and accelerate degradation reactions under light irradiation, offering a sustainable and energy-efficient approach to wastewater treatment.Numerous studies have explored the application of nickel oxide nanoparticles for the degradation of various classes of organic dyes, including azo dyes, anthraquinone dyes, and triarylmethane dyes [9].

Given the benefits associated with quaternary photocatalysts and their significance in advanced oxidation processes (AOPs), we present the synthesis, characterization, and application of a novel quaternary photocatalyst, $Co_3BaNiO_6$for the removal of dyes from wastewater. Toluidine blue dye serves as the model pollutant in this study.

II. Experimental

Materials and Method

Barium chloride, cobalt chloride, and nickel chloride served as precursor materials (sourced from Merck) in the synthesis of the photocatalyst, while sodium hydroxide from CDH was employed as the precipitating agent. Toluidine blue functioned as the model pollutant in the study. To adjust the pH of the solutions, hydrochloric acid (CDH) and sodium hydroxide (CDH) were utilized, with pH measurements conducted using a pH meter (Hena, imported pen type). UV-Vis spectrophotometry (CHINO) was employed for kinetic study to record the optical density of solutions at various time intervals. For irradiation, a 200 Watttungstenlamp (Philips) was utilized, and light intensity was measured using a solarimeter (CEL-201). Scavengers, namely Isopropanol was incorporated to trap active species.All chemicals were utilized in their LR grade, with a purity range of approximately 95-99%.

The solid co-precipitation method was employed, and controlled conditions were maintained during the process. 0.1 M solutions of each, Barium chloride, cobalt chloride, and nickel chloride were prepared and pH was recorded as 4.1, 5.2, and 4.5 respectively. All the three solutions were mixedto attain the pH 5.4. The mixture was stirred for 2 hours and while stirring, 5N NaOH solution was added drop by drop for precipitation to obtain white colored material. This was then stirred for half an hour and then allowed to settle down. Temperature during the process was maintained at 26℃. Supernatant liquid was checked for further precipitation, filtered and dried in a microwave oven at 200℃. White solid was obtained with yield 51g and the yield percentage was 76.6 %. This was then subjected to calcination at 500℃ for 3 hours. The color of the prepared solid changed to brownish black with yield of 40.3 g and the yield percentage was 60.6 %.,

For kinetic study, solution of Toluidine Blue dye (TB) was taken in a borosil beaker, pH was measured and photocatalyst was added. It was then exposed to light and after certain time intervals, optical density (OD) was recorded. A plot of log optical density (O.D.) verses time was straight line suggesting that the reaction of degradation follows pseudo first order kinetic law (figure 7).

***Instrumentation**:*

The elemental composition of the sample was studied by an energy-dispersive X-ray analyzer (JSM7600F (Jeol)) and X-ray diffractometer model (D8 DISCOVER (Bruker) IITGN Instruments INDIA) was used for XRD analysis of nanoparticles. FE-SEM and EDS was carried on Brunker (MAG: 10000×HV:15kV) for crystal images and elemental study. Elemental composition as well as the chemical and electronic state of the atoms withinthe nanomaterial were confirmed by XPS model (PHI 5000 VersaProbe III, IIT Roorkee). UV-Vis study for calculation of band gap was carried on Hitachi 330 spectrophotometer (running perkinElmer UV winLab 6.0.3.0730/1.61.00).

The absorbance of the dye was measured using a UV–Vis spectrophotometer (CHINO).Using the following formula, the degradation percentage of the dyewas calculated:

Percent degradation = $\frac{Co-C}{Co} X\ 100$

Where, C_o and C represent the initial concentration and final concentration of the dye at different time intervals, respectively.

III. Result And Discussion

The resulting brownish black-colored material was obtained with a yield of 71.73% after calcination. The larger band gap (4.3 eV) contributed to higher photo-quantum efficiency, ensuring prolonged lifetime of photo-generated electrons and holes for effective pollutant degradation. Characterization of the prepared photocatalyst by various analytical methods and photocatalytic degradation process with mechanism are discussed here in.

Element composition study:

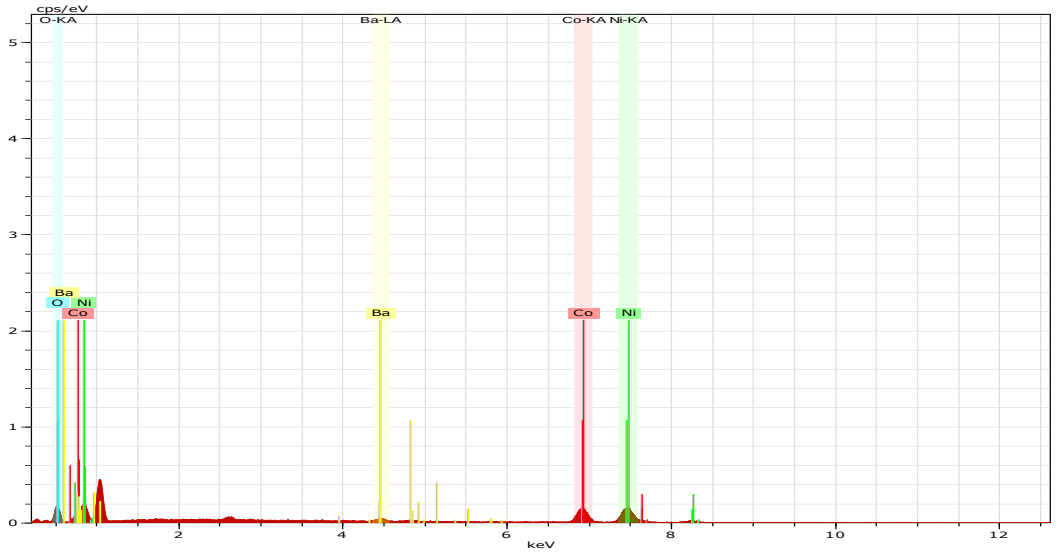

Figure 1: EDS spectra of Co_3BaNiO_6

Table no1: Elemental Composition

Element	Weight%	Atomic%
Ba (L)	61.39	34.95
Co (K)	25.73	34.05
Ni(K)	08.93	11.81
O(K)	03.93	19.13
Totals	100.00	

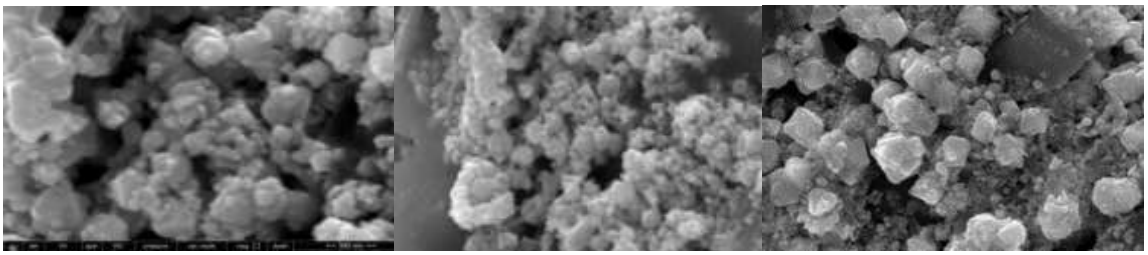

Figure 2: FESEM crystal images

The EDS spectrum of Co_3BaNiO_6 NPs is shown in Figure1 and the weight % as well as the atomic % of the elements is given in Table 1 which confirms the synthesis ofCo_3BaNiO_6NPs.A strong band for Ba, Co, Ni and O each with elemental weight percent of 61.39, 25.73, 8.93 and 3.93 respectively are observed.

The surface morphological nature of the prepared nonmaterial is analyzed by FESEM micrographs and the obtained image is shown in Figure 2. It is seen from the FESEM image that nonmaterial has an agglomerated spherical-like morphology.

Elemental ratio study:

The chemical composition and elemental constituents of the nanomaterial were investigated through X-ray Photoelectron Spectroscopy (XPS) analysis, with the corresponding spectrum depicted in Figure 3 showing a strong band for Ba, Co, Ni and O each with elementalratio of 3:1:1:4. In Figure 3(a), the XPS spectrum of the synthesized nanomaterial revealed distinct peaks at 780 eV and 795 eV, corresponding to Co $2p_{3/2}$. This observation suggests the presence of Cobalt ions in oxidation states of +3 and +2 [10]. Subsequently, in Figure 3(b), the spectrum exhibited peaks at 780.1 eV and 795.72 eV, corresponding to Ba $3d_{5/2}$ and respectively, indicating Ba in an oxidation state of +2 and the presence of BaO [11]. Figure 3(c) illustrates single peaks at a binding energy of 853 eV, attributed to Ni $2p_{3/2}$, confirming the presence of Ni ions in the +2oxidation state, suggestive of the presence of Ni as NiO [12]. Additionally, XPS analysis of O1s, as depicted in Figure 3(d), displayed a broad peak ranging from 531.23 eV to 533.27 eV, associated with oxygen vacancies and adventitious hydroxyls of water adsorbed on the oxide surface under ambient conditions [13]. This observation underscores the susceptibility of mixed metal oxide material or catalyst affirming the molecular formula as Co_2O_3.CoO.BaO.NiO and containing surface oxygen vacancies to oxidation upon exposure to ambient conditions, due to the strong adsorption energy of water.

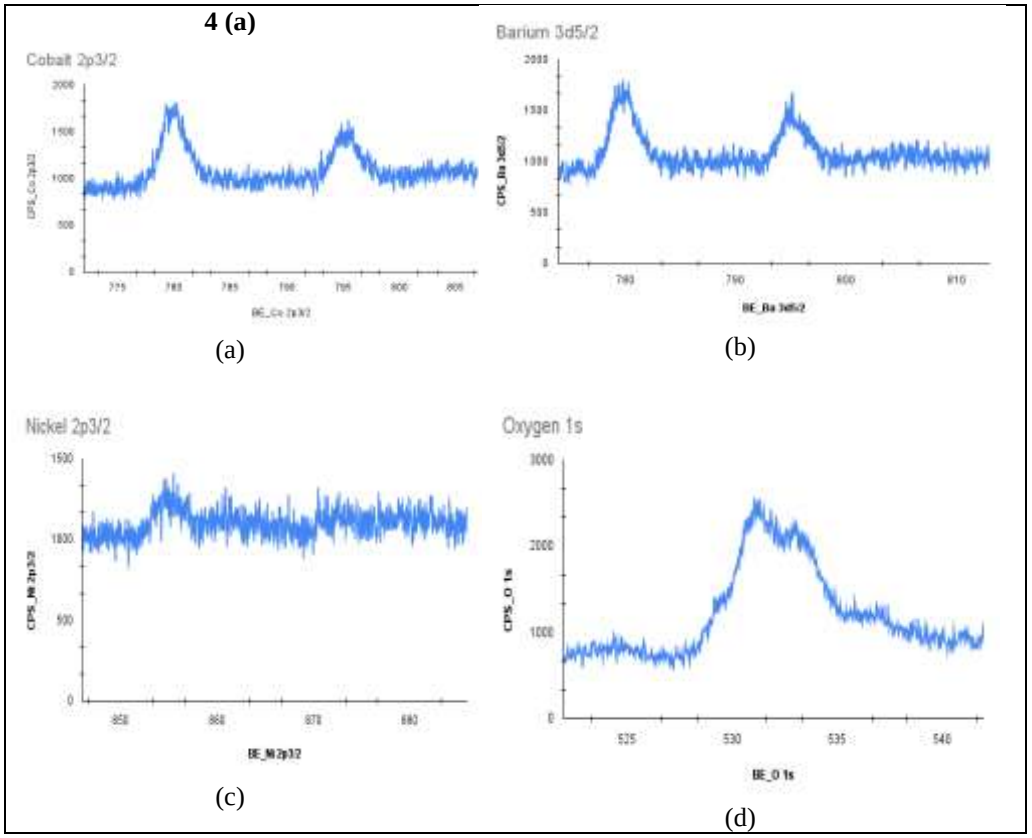

Figure 3: XPS Spectrum of Nanoparticles

Crystal size calculation:

The X-ray diffraction (XRD) analysis of Co_3BaNiO_6NPs is illustrated in Figure 4. Notably, diffraction peaks manifest at angular positions of 20.22°, 26.61°, 31.01°, 32.00°, and 45.71° for Co_3BaNiO_6, corresponding to the crystallographic planes (101), (110), (111), (113), and (103) respectively, as cited in previous research. The determination of the average grain size is conducted by evaluating the peak widths, with particular consideration given to the most intense peak 32.00° (113). This evaluation employs the Debye–Scherrer equation:

$D = (k\lambda / \beta \cos \theta)$

The calculated average crystallite size of the pure $Co_3BaNiO_6$is found to be 43.82 nm. Table 2 represents the FWHM values obtained by XRD.

Table no2: XRD FWHM values of the nanoparticles

Peak position (2θ theta)	FWHM Values	D(nm)
20.2230	0.3542	23.81
26.6122	0.3542	24.080
31.0158	0.2362	36.471
32.0042	0.1476	58.518
45.7134	0.1181	76.270
Average D Value	**43.82**	

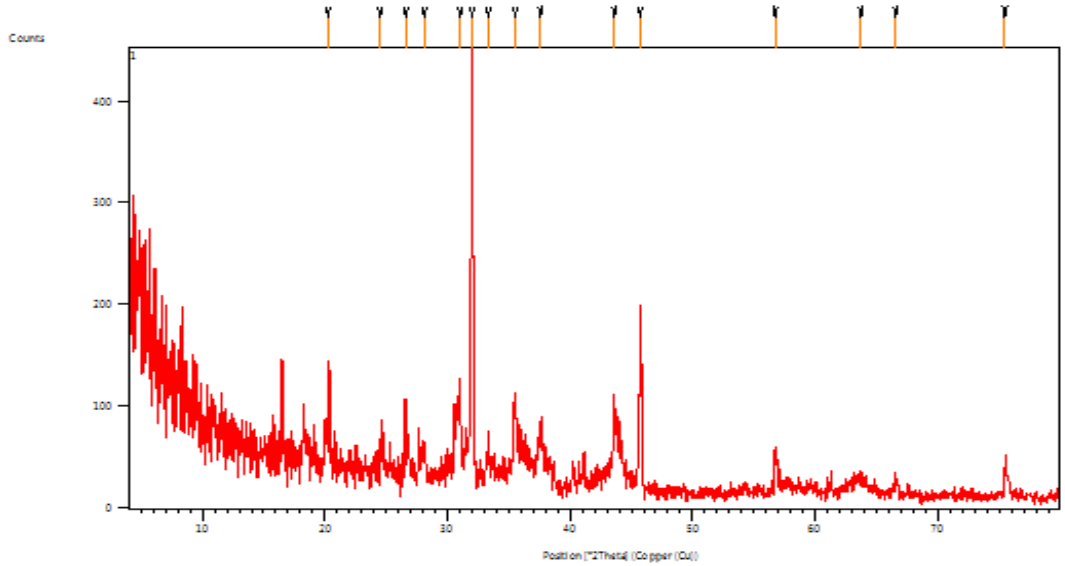

Figure 4: XRD pattern of Photocatalyst

Band gap calculation:

The optical properties of the nanomaterial were recorded by using the UV–Vis absorption spectrophotometer and are shown in figure 5. The absorption coefficient (α) is calculated using:

$\alpha=2.303A/t$

Where, A = absorbent; t= sample thickness

The bandgap energy is calculated by extrapolating the linear part of the graph between $(\alpha h\nu)^2$a.u. and photon energy (hν), until it meets the x-axis [32] and is shown in figure 6.UV–Vis spectroscopy revealed a peak absorbance at 232nm, with an optical bandgap estimated to be ≈4.3eV.

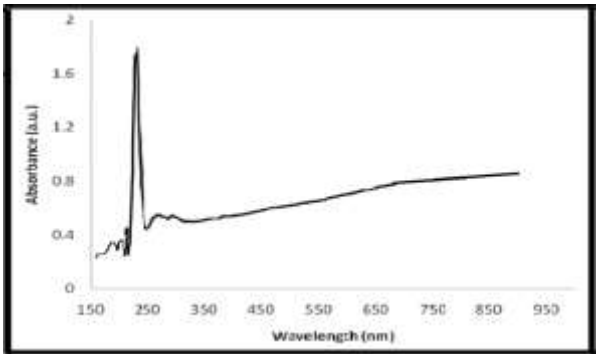

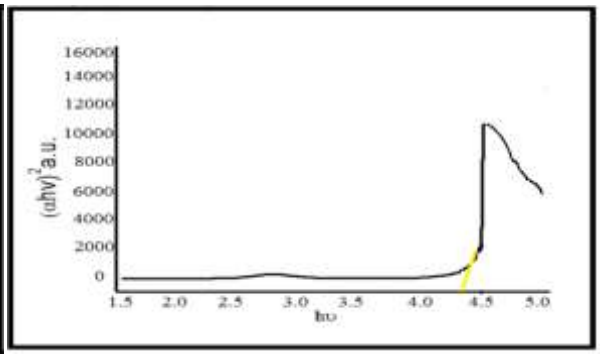

Figure 5: UV-VIS spectra peak absorption **Figure 6: UV-VIS spectra for bandgap**

Photocatalytic activity of Co_3BaNiO_6nanoparticles:

A straight line was observed in the plot of 1+ log of optical density (O.D.) and time during the reaction and is shown in Figure 7. Different models were studied to understand the degradation process, like pseudo-

first-order and pseudo-second-order (Type-1, Type-2, Type-3, Type-4, and Type-5). After analyzing the data, it was observed that the pseudo-first-order model best explains the degradation [14].Theoptimized conditions for break down TB were at a pH of 10.5 using 0.18 g of photocatalyst, having the dye concentration of 0.4×10^{-4} M, and a light intensity of 1640 mW/cm^2. Thus,careful control of these factors becomes the key to effective removal of dyes.

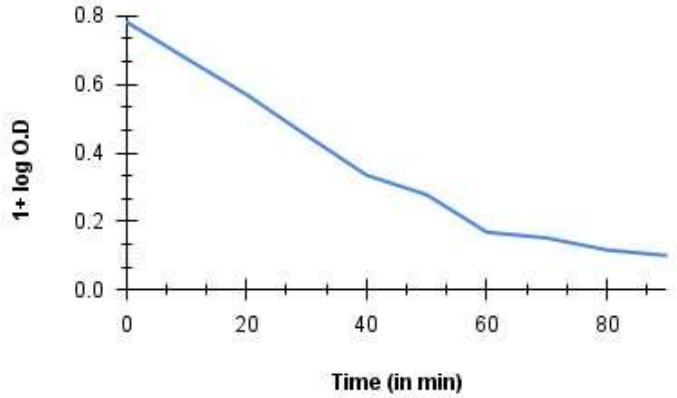

Figure7: Photo Catalytic activity of $Co_3NiBaO_6$for degradation of TB

A typical run

Effect of pH:

The degradation rate of the dye is significantly influenced by the pH of the solution, given the sensitivity of dyes to pH variations. Some dyes undergo a change in color with alterations in pH. To explore this impact, the pH of the solution was systematically varied while keeping all other factors constant. Notably, the initial optical density of the solution exhibited changes corresponding to variations in pH, as evident in multiline graphs. The study delved into the pH range of 6.0 to 10.5 with maximum rate at 10.5 and the outcomes are illustrated in Figure 8. This comprehensive analysis sheds light on how pH acts as a pivotal factor in influencing the degradation process of the dye. It was observed that rate of photocatalytic degradation increased with increase in pH.

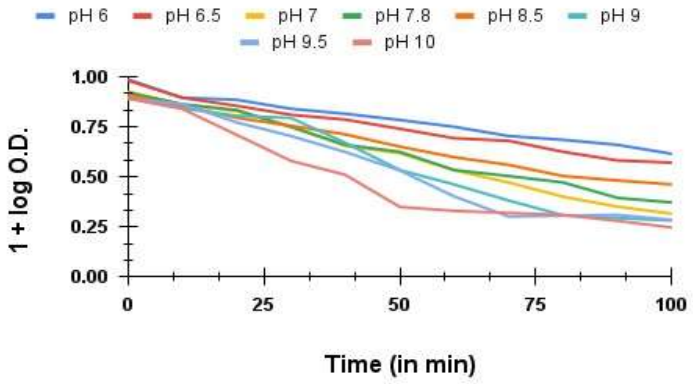

Figure 8: Photodegradation of TB on Co_3BaNiO_6at different pH

The increase in pH increases photocatalytic degradation and can be explained on basis of theeffectofsurfacecharge. At higher pH values, surfaces tend to become more negatively charged, which enhances the adsorption of positively charged dye molecules due to electrostatic attraction. simultaneously generation of electron hole pair tends to generate hydroxyl radicals which are key reactive species responsible for the degradation of TB. At higher pH values, the concentration of hydroxide ions (OH^-) in the solution increases. These hydroxide ions react with photogenerated holes (h+) on the photocatalyst surface to produce more hydroxyl radicals. Therefore, higher pH leads to increased generation of hydroxyl radicals, enhancing the degradation of dye [15].

Effect of photocatalyst doses:

The impact of the photocatalyst dose on the degradation process was systematically examined by varying its weight, while keeping all other factors constant. Figure 9 vividly illustrates the effects of this variation.Remarkably the maximum rate of degradation was observed at a photocatalyst dose of 0.18 g and is explained as availability of more surface area to absorb light radiations and generate greater number of electron hole pairs. This phenomenon is attributed to the fact that an elevated dose of photocatalyst results in an increased surface area of particles exposed to light [15].However, as the dose of the photocatalyst was further increased, an interesting observation unfolded, the rate of the reaction began to decrease and is due to recombination of electrons and holes due to their enhanced quantity.

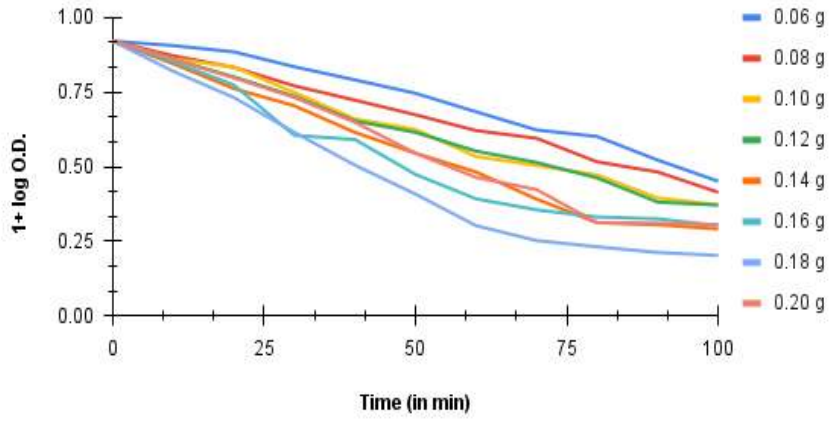

Figure 9: Photodegradation of TB on Co_3BaNiO_6at different photocatalyst Dosage (g)

Effect of dye concentration:

Thestudy was carried between the range of $2.5\times10^{-5}$to 1×10^{-4} M of dye concentration with keeping all other factors constant and data are represented in figure 10. Observations revealthatrateofreactionincreaseswithincreaseinconcentrationofdye as more dye molecules are available to absorb photons from light and get excited. After attaining maximum value (at 0.4 x 10^{-4} M), increase in concentration of thedye decreases the rate of degradation as beyond the concentration, addition of dye imparts darker colorto the reaction mixture and starts acting as filter to the incident light.

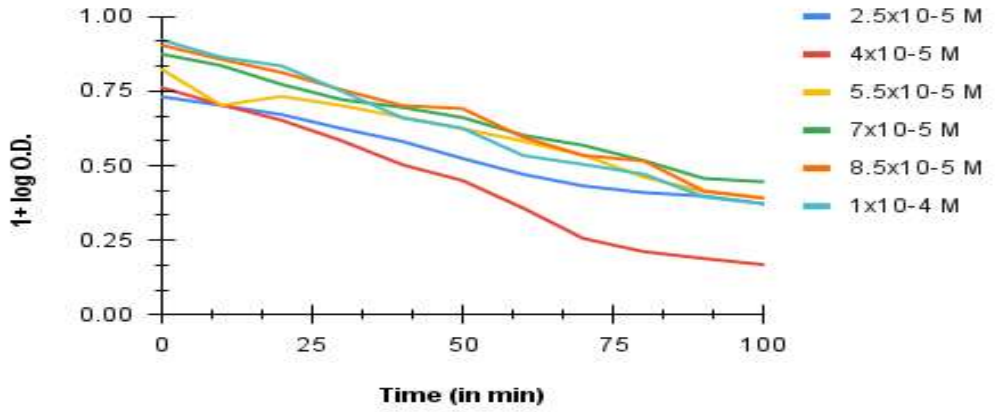

Figure 10:Photodegradation of TB on Co_3BaNiO_6at different Concentrations of Dye (M)

Effect of intensity of light:

The experiment involved varying the light intensity within the range of 1320 to 1740 mW/cm² and the corresponding data are visually depicted in figures 11. All other experimental parameters were maintained at a constant level.

It was observed that the rate of photocatalytic degradation exhibited an increment corresponding to the increase in light intensity. This phenomenon is rationalized by the heightened number of photons striking per unit area per unit time as the light intensity increases. Consequently, there is an augmentation in the population of excited dye molecules and electron-hole pairs at the surface of the photocatalyst. The maximum rate of

degradation was identified at a light intensity of1640 mW/cm² and then decrease because at higher light intensities, there may be an increased likelihood of recombination of photogenerated electron-hole pairs. This recombination process can reduce the number of reactive species available for dye degradation, contributing to a decrease in efficiency.

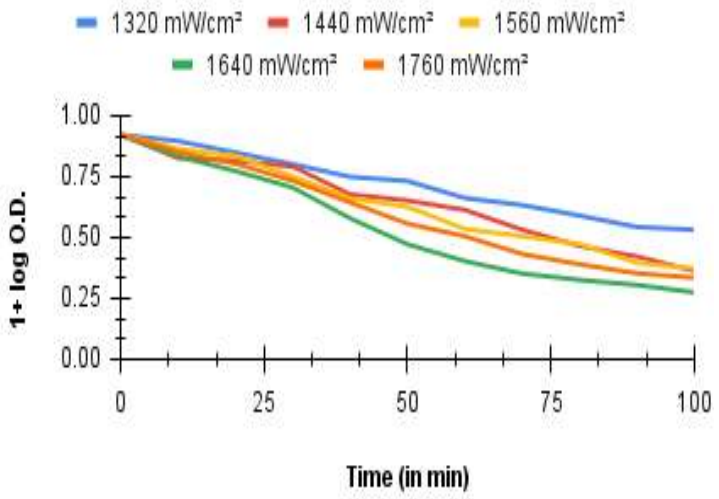

Figure 11: Photodegradation of TB on Co_3BaNiO_6at different Intensities of Light (in mW/cm^2)

Ascertaining the reactive species:

Numerous scavengers are used to study the participation of reactive species in the degradation reaction. Isopropanol is one of them which scavenges OH free radicals. The degradation of TB dye with the nanomaterial Co_3BaNiO_6in presence of 5 ml isopropanol was carried out (Figure 12). The degradation became constant and only 15% dye was degraded. Isopropanol scavenges the reactive oxygen species (ROS),that is hydroxyl radicals (•OH). Iteffectively captures the holes preventing them from participating in the degradation process therefore, disrupting the photocatalytic degradation process, leading to the cessation of dye degradation [31].

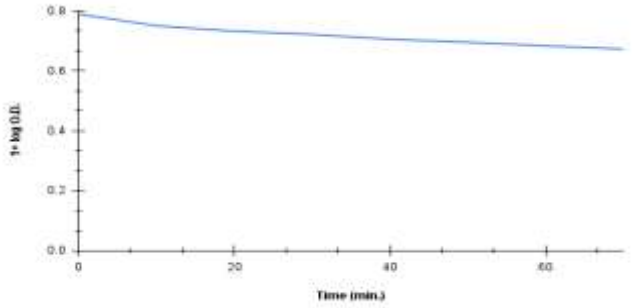

Figure 12: Effect of Scavenger on Dye Degradation

Possible mechanism is thus proposed here:

$MO + h\nu \rightarrow MO (h^+ + e^-)$ ……..……....(1)

MO = Metal oxide

Oxidative reactions due to photocatalytic effect:

$h^+ + H_2O \rightarrow H^+ + {}^{\bullet}OH$ ……..…..(2)

$2\ h^+ + 2\ H_2O \rightarrow 2H^+ + H_2O_2$ ……...…..…..…(3)

$H_2O_2 \rightarrow 2\ {}^{\bullet}OH$ ……(4)

Reductive reactions due to photocatalytic effect:

$e^- + O_2 \rightarrow {}^{\bullet}O_2^-$ ……..……...(5)

${}^{\bullet}O_2^- + H_2O + H^+ \rightarrow H_2O_2 + O_2$ ……(6)

$H_2O_2 \rightarrow 2\ {}^{\bullet}OH$ ……....(7)

Isopropanol scavenges these hydroxyl radicals and ceases the reaction completely [33]

Recycling of the photocatalyst

The \recovered photocatalyst was recycled i.e. washed and calcined again. This was then used for degradation of TB and it was observed that its efficiency remained unaltered even after its repeated use for next five cycles. This property makes it more valuable to be used as potential photocatalyst in environmental remediation.

IV. Conclusion:

The synthesis of Co_3BaNiO_6 nanoparticles via co-precipitation method was successfully carried out. The yield efficiency was 60.6 % after calcination. Comprehensive characterization through X-ray diffraction (XRD), field-emission scanning electron microscopy (FE-SEM), energy-dispersive X-ray spectroscopy (EDS), X-ray photoelectron spectroscopy (XPS), and UV-visible (UV-VIS) spectroscopy has revealed detailed insights into the structure and morphology of the nanoparticles. With an average crystallite size of 43.82 nm, the nanoparticles exhibit favorable characteristics for catalytic applications. The as-prepared photocatalyst demonstrates remarkable efficacy in the photodegradation of Toluidine Blue (TB) dye in aqueous medium. The photodegradation efficiency shows a direct correlation with the catalyst dosage, reaching an optimal level before plateauing. Moreover, the photodegradation rate exhibits sensitivity to variations in initial dye concentration, pH levels, and light intensity. Specifically, enhanced photodegradation rates are observed at lower initial dye concentrations, elevated pH levels, and increased light intensities, underscoring the versatility and potential of the synthesized photocatalyst for environmental remediation applications.

Reference

[1] H.P. Shivaraju, G. Midhun, K.M. Anil Kumar, S. Pallavi, N. Pallavi & S. Behzad, Degradation Of Selected Industrial Dyes Using Mg-Doped Tio_2 Poly Scales Under Natural Sunlight As An Alternative Driving Energy, Applied Water Science, 7, 2017, 3937-3948.

[2] M. Das & K.G. Bhattacharyya, Oxidation Of Rhodamine B In Aqueous Medium In Ambient Conditions With Raw And Acid-Activated Mno_2, Nio, Zno As Catalysts, Journal Of Molecular Catalysis A: Chemical, 391, 2014, 121-129.

[3] S.I. Kaya, M. Yence, G. Ozcelikay, A. Cetinkaya, F. Budak & S.A. Ozkan, Development Of 2d Nanomaterials-Based Sensors For Detection Of Toxic Environmental Pollutants, In Two-Dimensional Materials For Environmental Applications, 2023, 269-297.

[4] R. Rashid, I. Shafiq, P. Akhter, M.J. Iqbal & M. Hussain, A State-Of-The-Art Review On Wastewater Treatment Techniques: The Effectiveness Of Adsorption Method, Environmental Science And Pollution Research, 28, 2021, 9050-9066.

[5] B. Prelot, I. Ayed, F. Marchandeau& J. Zajac, On The Real Performance Of Cation Exchange Resins In Wastewater Treatment Under Conditions Of Cation Competition: The Case Of Heavy Metal Pollution, Environmental Science And Pollution Research, 21, 2014, 9334-9343.

[6] B. Gomez-Ruiz, S. Gómez-Lavín, N. Diban, V. Boiteux, A. Colin, X. Dauchy & A. Urtiaga, Efficient Electrochemical Degradation Of Poly-And Perfluoroalkyl Substances (Pfass) From The Effluents Of An Industrial Wastewater Treatment Plant, Chemical Engineering Journal, 322, 2017, 196-204.

[7] B.D. Tripathi & S.C. Shukla, Biological Treatment Of Wastewater By Selected Aquatic Plants, Environmental Pollution, 69, 1991, 69-78.

[8] P.R. Kiezyk& D. Mackay, Waste Water Treatment By Solvent Extraction, The Canadian Journal Of Chemical Engineering, 49, 1971, 747-752.

[9] J.A. Garrido-Cardenas, B. Esteban-García, A. Agüera, J.A. Sánchez-Pérez & F. Manzano-Agugliaro, Wastewater Treatment By Advanced Oxidation Process And Their Worldwide Research Trends, International Journal Of Environmental Research And Public Health, 17, 2020, 170.

[10] R.S. Dobson & J.E. Burgess, Biological Treatment Of Precious Metal Refinery Wastewater: A Review, Minerals Engineering, 20, 2007, 519-532.

[11] S. Gupta, R. Fernandes, R. Patel, M. Spreitzer & N. Patel, A Review Of Cobalt-Based Catalysts For Sustainable Energy And Environmental Applications, Applied Catalysis A: General, 2023, 119254.

[12] M.A. Ansari & N. Jahan, Structural And Optical Properties Of Bao Nanoparticles Synthesized By Facile Co-Precipitation Method, Materials Highlights, 2, 2021, 23-28.

[13] A.K. Bhakta, S. Kumari, S. Hussain, P.C. Pais, P. Martis, R.J. Mascarenhas & Z. Mekhalif, Methylene Blue Dye Removal Through Adsorption Onto Amorphous Bao Nanoparticles Decorated Mwcnts, Materials Research And Applications: Select Papers From Jch8-2019, 2021, 231-240.

[14] F. Naz & K. Saeed, Synthesis Of Barium Oxide Nanoparticles And Its Novel Application As A Catalyst For The Photodegradation Of Malachite Green Dye, Applied Water Science, 12, 2022, 121.

[15] A. Akbari, Z. Sabouri, H.A. Hosseini, A. Hashemzadeh, M. Khatami & M. Darroudi, Effect Of Nickel Oxide Nanoparticles As A Photocatalyst In Dyes Degradation And Evaluation Of Effective Parameters In Their Removal From Aqueous Environments, Inorganic Chemistry Communications, 2020, 107867.

[16] H.P.P. La, T.K. Truong & V. Van Pham, Electrochemical Water Splitting Of 3d Binder-Free Hydrothermally Synthesized Co3o4/Unidirectional Carbon Cloth, Environmental Science And Pollution Research, 2023, 1-10.

[17] M. Salavati-Niasari, A. Khansari & F. Davar, Synthesis And Characterization Of Cobalt Oxide Nanoparticles By Thermal Treatment Process, Inorganicachimica Acta, 362, 2009, 4937-4942.

[18] J.T. Verhoeven & H. Van Doveren, Xps Studies On Ba, Bao And The Oxidation Of Ba, Applications Of Surface Science, 5, 1980, 361-373.

[19] A.Z. Bazeera& M.I. Amrin, Synthesis And Characterization Of Barium Oxide Nanoparticles, Iosr J. Appl. Phys., 1, 2017, 76-80.
[20] W. Huang, S. Ding, Y. Chen, W. Hao, X. Lai& J. Peng, 3d Nio Hollow Sphere/Reduced Graphene Oxide Composite For High-Performance Glucose Biosensor, Scientific Reports, 7, 2017, 5220.
[21] S.S. Narender, V.V.S. Varma, C.S. Srikar, J. Ruchitha, P.A. Varma & B.V.S. Praveen, Nickel Oxide Nanoparticles: A Brief Review Of Their Synthesis, Characterization, And Applications, Chemical Engineering & Technology, 45, 2022, 397-409.
[22] H. Idriss, On The Wrong Assignment Of The Xps O1s Signal At 531–532 Ev Attributed To Oxygen Vacancies In Photo-And Electro-Catalysts For Water Splitting And Other Materials Applications, Surface Science, 712, 2021, 121894.
[23] F.M.F. De Groot, M. Abbate, J. Van Elp, G.A. Sawatzky, Y.J. Ma& C.T. Chen, Oxygen 1s And Cobalt 2p X-Ray Absorption Of Cobalt Oxides, Journal Of Physics: Condensed Matter, 5, 1993, 2277.
[24] E.D. Revellame, D.L. Fortela, W. Sharp, R. Hernandez & M.E. Zappi, Adsorption Kinetic Modeling Using Pseudo-First Order And Pseudo-Second Order Rate Laws: A Review, Cleaner Engineering And Technology, 1, 2020, 100032.
[25] N.F. Jaafara, A.A. Jalilb, S. Triwahyonoa, A. Ripinb& M.W. Alia, Significant Effect Of Ph On Photocatalytic Degradation Of Organic Pollutants Using Semiconductor Catalysts, Catalyst, 2, 2016.
[26] C. Fernández, M.S. Larrechi& M.P. Callao, Study Of The Influential Factors In The Simultaneous Photocatalytic Degradation Process Of Three Textile Dyes, Talanta, 79, 2009, 1292-1297.
[27] H.A.M. Salim & S.A.M. Salih, Photodegradation Study Of Toluidine Blue Dye In Aqueous Solution Using Magnesium Oxide As A Photocatalyst, International Journal Of Chemistry, 7, 2015, 143.
[28] C.S. Uyguner& M. Bekbolet, Photocatalytic Degradation Of Natural Organic Matter: Kinetic Considerations And Light Intensity Dependence, International Journal Of Photoenergy, 6, 2004, 73-80.
[29] A. Ahmadian, S. Ahmadi & B.A. Goharrizi, Roles Of Reactive Species In Photocatalysis: Effect Of Scavengers And Inorganic Ions On Dye Removal From Wastewater, International Journal Of Environmental Science And Technology, 20, 2023, 6433-6448.
[30] J.S.G. Neto, S. Satyro, E.M. Saggioro& M. Dezotti, Investigation Of Mechanism And Kinetics In The Tio_2 Photocatalytic Degradation Of Indigo Carmine Dye Using Radical Scavengers, International Journal Of Environmental Science And Technology, 18, 2021, 163.
[31] T. T. D. Nguyen, D. Nguyen, P. P. Vo, H. N. Doan, Pham, H. T. N. Hoang & P. T. Nguyen, The Roles Of Ethanol And Isopropanol As Hole Scavengers In The Photoreduction Reaction Of Graphene Oxide By Tio_2: A Competition Of Oxygenated Groups Removal And Carbon Defects Invasion. Journal Of Molecular Liquids, 381,2023, 121831.
[32] G. Sharma, A. Kumar, S. Sharma, M. Naushad, P. Dhiman, D. V. N. Vo, & F. J., Stadler, Fe_3o_4/Zno/Si_3n_4nanocomposite Based Photocatalyst For The Degradation Of Dyes From Aqueous Solution. Materials Letters, 278, 2020, 128359.
[33] 33. Lou, W., Kane, A., Wolbert, D., Rtimi, S. & Assadi, A. A., Study Of A Photocatalytic Process For Removal Of Antibiotics From Wastewater In A Falling Film Photoreactor: Scavenger Study And Process Intensification Feasibility. Chemical Engineering And Processing: Process Intensification, 122, 2017, 213-221.